Supplementary Materials for

Stretchable, Transparent, Ionic Conductors

Christoph Keplinger[1,2,3†], Jeong-Yun Sun[1,2†], Choon Chiang Foo[1,2,4], Philipp Rothemund[1,2], George M. Whitesides[2,3,5*], and Zhigang Suo[1,2*]

[1]School of Engineering and Applied Sciences, Harvard University, Cambridge, MA 02138, USA.
[2]Kavli Institute for Bionano Science and Technology, Harvard University, Cambridge MA 02138, USA.
[3]Department of Chemistry and Chemical Biology, Harvard University, Cambridge, MA 02138, USA.
[4]Institute of High Performance Computing, 1 Fusionopolis Way, Singapore 138632
[5]Wyss Institute for Biologically Inspired Engineering, , Harvard University, Cambridge MA 02138, USA.

[†] These authors contributed equally to this work.

* correspondence to: GWhitesides@gmwgroup.harvard.edu, suo@seas.harvard.edu

This PDF file includes:

Other Supplementary Material for this manuscript includes the following:

Materials and Experimental Methods

Materials. Unless otherwise specified, experiments were carried out using copper as the electrode, VHB 4910 (3M) as the dielectric, and NaCl-containing polyacrylamide hydrogel as the electrolyte.

The hydrogel was synthesized using acrylamide (AAm; Sigma, A8887) as monomers, N,N-methylenebisacrylamide (MBAA; Sigma, M7279) as crosslinkers, ammonium persulfate (AP; Sigma, A9164) as photo initiator, and N,N,N',N'-tetramethylethylenediamine (TEMED; Sigma, T7024) as crosslinking accelerator.

AAm and NaCl were dissolved in deionized water, with AAm fixed at 2.2 M, but NaCl varied from 1.37 to 5.48 M. Also added were MBAA 0.0006 the weight of AAm, and AP 0.0017 the weight of AAm. After degassing in a vacuum chamber, TEMED 0.0025 the weight of AAm was added. The solutions were poured into a 100.0 x 100.0 x 0.1 mm^3 glass mold, and covered with a 3 mm thick glass plate. The gels were cured using an ultraviolet light crosslinker (UVC 500, Hoefer) for 20 min with power 8 W and 254 nm wavelength.

The gels were cut into the designed shape by using a laser cutter (VersaLaser VLS3.50, Universal Laser Systems) with a power of 50 W and a speed of 14 cm/sec.

Dielectric elastomer actuators were also fabricated using two other types of conductors: carbon grease (MG Chemicals Carbon Conductive Grease: 846-80G), and an ionic liquid (1-Decyl-3-methylimidazolium chloride, $[C_{10}MIM][Cl]$; Sigma, 690597).

Transparent actuator. VHB has been marketed as adhesive tapes; this property played a significant role in the fabrication of the devices. The actuator involved layered electrolytic and dielectric elastomers (Fig. S1). We used fairly thick (100 μm) hydrogel to slow drying. To minimize the elastic constraint of hydrogels, we stacked

three layers of the VHB. The layers of VHB were stretched radially to three times the initial radius, and fixed to a circular rigid frame made of an acrylic, inner radius 4 cm for the circular hydrogel and 8 cm for the heart-shaped hydrogel. Before the hydrogel was stacked onto the dielectric, the surface of the hydrogel was dried with nitrogen gas. The removal of water on the surface of the hydrogel enhanced the adhesion between the hydrogel and the dielectric.

We characterized actuators with hydrogels of circular shape. The radius of the hydrogels was ¼ the radius of the rigid frame, and hydrogels containing 2.74 M NaCl were used. Voltage was generated using a high-voltage amplifier (Model 50/12, TREK) and a function generator. The movements of the hydrogels were recorded using a high-speed camera (Vision Research Phantom V310).

When the voltage was suddenly applied and was held constant subsequently, the actuator deformed as a function of time, and the rate of expansion became small after about 20 s (Fig. S2). The expansion in area at 20 s was recorded as a function of the applied voltage. The voltage-induced strain was limited by electromechanical instability, and the elasticity of the hydrogels did not appreciably constrain the dielectric (Fig. S3); see the theoretical analysis below.

When the voltage was cycled at a certain frequency, the actuator oscillated. The initial cycles were not steady; the amplitude of the oscillating actuator changed from cycle to cycle. After some cycles the actuator oscillated steadily, and the relative change between the maximum and minimum areas defined the area strain. We determined the area strain as the voltage cycled between steps of 0 and 18 kV, at frequency ranging from 0.05 to 1024 Hz (Fig. 2F).

Movies were recorded with frame rates from 1000 up to 3200 frames per second. To obtain the electrode area single frames of the videos were analyzed with ImageJ. A

LED connected to the sync output of the function generator was placed at the corner of the recorded scene to indicate voltage on and off in the video.

In these demonstrations we used relatively thick layers to make material handling easy, and to demonstrate the high-voltage capability of the design. In many practical devices, one may wish to scale down the thickness and voltage.

Actuators were also made using carbon grease as conductors. The actuators were subject to cyclic voltage, and the area strains were recorded. This response of the actuators using carbon grease as the conductor is nearly indistinguishable from that of actuators using the hydrogel as the conductor (Fig. S4).

Transparent loudspeaker. The fabrication process was similar to that of the transparent actuator, but with different dimensions. Three layers of the VHB 4910 were stacked together, stretched to three times the initial radius, and fixed to a circular acrylic frame of radius 10 cm. Hydrogels of radius 5 cm were attached to the surfaces of the dielectric.

The transparent loudspeaker was placed in front of a laptop, which was playing a music video (Fig. S5). The sound of the music was fed to the loudspeaker as analog electrical signal, from the audio output of the laptop, through a high-voltage amplifier (TREK, model 30/20A; fixed 3000 V/V gain; slew rate larger than 750 V/μs). The electric field deforms the dielectric elastomer by the Maxwell stress, which is quadratic in voltage. To preserve the polarity of the analog electrical signal and prevent frequency doubling, the high voltage amplifier was also programmed to add a 12.5 kV DC offset. The offset also shifted the time-varying signal up, to the region just below the dielectric strength of the elastomer, where the electromechanical coupling was strongest. This high voltage signal was applied to the hydrogel layers. A webcam with a microphone (electromagnetically shielded with a grounded metallic mesh; webcam model: Logitech,

QuickCam® Pro 9000) recorded the scene from 15 cm distance. The sound produced from the transparent loudspeaker was clearly audible from 5 m distance.

We study the fidelity of the sound reproduction by feeding the loudspeaker with a 20 s test signal (*31*). The signal was of constant amplitude and a linear sine sweep from 20 Hz to 20 kHz. The audio recordings of the video files were extracted in form of WAV (Waveform Audio File Format) files. Spectrograms of the WAV files were used to analyze the sound. The colors show the intensity distribution of frequencies as a function of time (Fig. 3). Warmer colors indicate higher intensity. The frequency spectrum at a given time was obtained by short-time Fourier transform of the WAV data.

Our transparent, stretchable loudspeaker was intended to illustrate the combination of three attributes of the layered electrolytic and dielectric elastomers: high voltage, a frequency bandwidth large enough to cover the entire audible range, and ultrahigh transparency. For commercial applications, such as transparent loudspeakers placed in front of screens or on windows, the resonance behavior has to be optimized by special frame constructions or alternative geometries. Lowering the membrane thicknesses and using multilayered electrolytic and dielectric elastomers will bring the required driving voltage down to practical levels.

Transmittance of elastomeric ionic hydrogels. Optical transmission spectra of the hydrogels were measured using a spectrophotometer (DU530, Beckman) with quartz cuvettes for the whole range of visible light. A quartz cuvette with pure water (≈ 99.99% transmittance at 550 nm) was used as a reference to reduce the reflection from index mismatch. Since the transmittance of the hydrogels is very high, normal spectrophotometer cannot measure the transmittance of layers of 100 μm thick hydrogels used in our devices. Therefore, a layer of 11 mm thick hydrogel containing 5.48 M of NaCl was used to measure the transmittance. The transmittance is defined as

$T=I/I_0$, where I is the intensity of the transmitted light, and I_0 is the intensity of the incident light. The transmittance was measured over the visible range of wavelengths (Fig. 4C).

The transmittance decreases as the thickness of the sample l increases, and is assumed to obey the Beer-Lambert law:

$$T = \exp(-\alpha l), \tag{1}$$

where α is the absorption coefficient of the hydrogel. This expression was used to convert the transmittance measured from the 11 mm thick hydrogel to the transmittance of the 100 μm thick hydrogel.

Resistance of elastomeric ionic hydrogels under stretch. The resistivity of the hydrogels was measured as the hydrogels were pulled by a uniaxial force. The resistance was measured by using four-point probes. To minimize the effect of ions built up on the surface of the probes, the resistance was measured with three relatively large voltages (20 ~ 50 V; electrochemical potentials are much smaller) and the corresponding currents after saturation. Hydrogels containing 1.37, 2.74 and 5.48 M of NaCl were used. When the hydrogels were not stretched, the measured molar conductivity was 120.19 Scm^2/mol, which was close to a reported value of 118.5 Scm^2/mol for aqueous solutions (*32*). The resistivity increased somewhat when the hydrogels were pulled (Fig. 4A).

To a first approximation, the resistivity of a hydrogel, ρ, may be taken to be a constant independent of the stretch λ under uniaxial force. We use this approximation to estimate the resistance as a function of the stretch. The hydrogel has length L and cross-sectional area A in the undeformed state, and has length λL and cross-sectional area A/λ in the deformed state. Here the hydrogel is taken to be incompressible. The resistance of the hydrogel is $R_0=\rho L/A$ in the undeformed state, and is $R=\rho L\lambda/(A/\lambda)$ in the deformed

state. Thus, the ratio of these two values of resistance is $R/R_0=\lambda^2$. This expression closely approximates the measured resistance of the hydrogel (Fig. 4B).

Ionic liquids as conductors for high-speed, large-strain dielectric elastomer actuators. Ionic liquids are nonvolatile electrolytes, and are being developed for applications including lithium-ion batteries, fuel cells and dye-sensitized solar cells (*33*). A large number of ionic liquids exists, and may be selected to suit specific applications. Furthermore, ionic liquids can be used as solvents to form ion gels, which are stretchable, transparent, ionic conductors (*19*). An example of using ionic liquids as conductors for dielectric elastomer actuators was given in a previous paper (*34*). By a combination of experiment and theory, here we demonstrate that ionic liquids can be used as conductors for high-speed, large-strain dielectric elastomer actuators.

We built an actuator using a commercially available ionic liquid 1-Decyl-3-methylimidazolium chloride, [C_{10}MIM][Cl]. One layer of VHB 4910 was stretched to three times the initial radius and fixed to a circular rigid acrylic frame of diameter 12 cm. The ionic liquid was painted to the two faces of the dielectric elastomer within circular regions of diameter 3 cm. On each face, a line of the ionic liquid was also painted from the circular region to the acrylic frame, where the line was connected to a copper electrode.

When a step voltage was applied, the actuator expanded gradually. The area strain at 20 s after the voltage is applied is plotted as a function of the magnitude of the voltage (Fig. S6A). When a cyclic voltage was applied, the steady area strain was recorded as a function of the frequency (Fig. S6B). Both characteristics are comparable to those observed for actuators using carbon grease as conductors.

The RC delay of the actuator using the ionic liquid as the conductor remains exceedingly small, so that the frequency of actuation is not limited by the electrical

resistance of the ionic liquid, but by the mechanical inertia. The RC delay can be estimated using Eqn. (8) derived in the section on theory below, $\tau \sim c_D A_D R$. Assuming representative values for the thickness $H \sim 10^{-3}$ m and resistivity $\rho \sim 10\ \Omega$m of the ionic liquid, we find that the sheet resistance is $R = 10^4\ \Omega$/sq. For representative values $c_D = 10^{-7}$ F/m^2 and $A_D = 10^{-3}$ m^2, we estimate that $\tau \sim 10^{-6}$ s. Even though the sheet resistance of the ionic liquid is two orders of magnitudes higher than that of the ionic hydrogels, high-speed actuation is nevertheless readily achieved.

Charge leakage through VHB when three types of conductors are used. Leakage of electrical charge carriers through a dielectric is an important characteristic of devices operating at large electrical fields. For example, charge leakage decreases the efficiency of a device, and may lead to premature failure. Here we quantify charge leakage through VHB when three types of conductors are used: carbon grease, a hydrogel (2.74 M NaCl-containing polyacrylamide), and an ionic liquid ([C_{10}MIM][Cl]).

A test sample was placed in a glass tank, in which air was replaced with argon to minimize the influence of ambient charged species (Fig. S7A). Temperature of the argon atmosphere was held constant at 22 °C and the oxygen content was monitored to ensure consistent experimental conditions. An electric field mill (AlphaLab, Inc.; Ultra Stable Surface DC Volt Meter) monitored the electrical potential of a metal plate without direct contact to minimize charge loss into experimental equipment. The metal plate shared the electrical potential of one side of the test sample, while the other side was grounded. A HV source (Model 50/12, TREK) was connected to the metal plate to charge the test sample up to a voltage of 1000 V. We disconnected the HV voltage source and measured the decay of the voltage down to a level of 1000 V/e (~ 368 V). The geometry of the test samples was identical to the samples used in Fig 2E, except that only one layer of VHB was used here. Due to unavoidable, small variations in the dimensions of the handmade

samples, we quantified differences in initial conditions by measuring the capacitance (C_0) immediately after fabrication.

The decays of voltage were recorded for samples using the three types of conductors, and each sample was tested three times (Fig. S7B-D). Some variations in the shape of the curve and the decay time were observed, but variations between different samples with the same type of electrode were on the same order as the observed differences between samples fabricated with different types of conductors.

The sample with the hydrogel as the conductor was retested after 24h of storage time in a high-humidity environment (Fig S7E). Surprisingly, the leakage process was slower compared to the initial result. The reason for the observation is unclear, but we observed that some water had evaporated from the hydrogel over night and thereby increased the concentration of salt.

Theory

Voltage across the electrode/electrolyte interface. The electrode/electrolyte interface forms an electrical double layer (EDL), and behaves like a capacitor when the voltage across the interface is sufficiently small (Fig. 1). The EDL and the dielectric are in series. Consequently, when voltage V is applied between the two electrodes, the two capacitors add the same amount of charge, Q. To estimate the behavior of the circuit, we assume that both capacitors are linear: $Q=C_{EDL}V_{EDL}$ and $Q=C_DV_D$, where C_{EDL} is the capacitance of the EDL, and C_D the capacitance of the dielectric. Thus,

$$C_{EDL}V_{EDL} = C_DV_D \ . \qquad (2)$$

The capacitance of the EDL is $C_{EDL}=c_{EDL}A_{EDL}$, where c_{EDL} is the capacitance per unit area of the EDL, and A_{EDL} the area of the EDL. The capacitance of the dielectric is $C_D=\varepsilon A_D/H_D$, where ε is the permittivity, A_D is the area of the dielectric, and H_D is the

thickness of the dielectric. Also note that $V_D=H_D E_D$, where E_D is the electric field in the dielectric. Rewrite (2) as

$$\frac{A_{EDL}}{A_D}=\frac{\varepsilon_D E_D}{c_{EDL} V_{EDL}}. \quad (3)$$

The electric field in the dielectric is limited by electrical breakdown field E_{EB}, while the voltage across the EDL is limited by the range within which electrochemical reaction is averted. For representative values $E_{EB}=10^8$ V/m, $\varepsilon_D=10^{-11}$ F/m, $c_{EDL}=10^{-1}$ F/m^2 and $V_{EDL}=1$ V, we find that $A_{EDL}/A_D=10^{-2}$. When the area of the electrode/electrolyte interface is sufficiently large, the device will be limited by the electrical breakdown of the dielectric, rather than by the electrochemical reaction at the EDL. If needed, the area of the electrode/electrolyte interface can be increased, for example, by using a porous electrode, similar to that used in a supercapacitor. The electrode/electrolyte interface may form thin layers of reaction products, so long as they are stable under a small voltage.

Time delay due to resistance and capacitance (RC delay). In layered electrolytic and dielectric elastomers (Fig. S1), the net capacitance C of the circuit is given by

$$\frac{1}{C}=\frac{2}{C_{EDL}}+\frac{1}{C_D}. \quad (4)$$

The capacitance of the EDL is proportional to the area of the electrode/electrolyte interface. The electrochemistry of this interface is expected to be similar to that of an interface between the electrode and an aqueous solution. The capacitance per unit area of the EDL is on the order $c_{EDL}\sim10^{-1}$ F/m^2 (*19*). The capacitance of the dielectric is proportional to the area of the dielectric. The capacitance per unit area of the dielectric is

$$c_{\mathrm{D}} = \frac{\varepsilon}{H_{\mathrm{D}}} \sim \frac{10^{-11}\ \mathrm{F/m}}{10^{-3}\ \mathrm{m}} = 10^{-8}\ \mathrm{F/m^2}, \tag{5}$$

where ε is the permittivity of the dielectric. So long as the area of the EDL is not excessively small compared to that of the dielectric, the capacitance of the EDL is much larger than that of the dielectric:

$$C_{\mathrm{EDL}} >> C_{\mathrm{D}}. \tag{6}$$

Consequently, the net capacitance of the circuit is dominated by the contribution of the dielectric, $C \approx C_{\mathrm{D}}$.

The time delay due to the capacitance of the dielectric and the resistance of the electrolyte is

$$\tau = RC. \tag{7}$$

Consequently, the *RC* time constant for the layered electrolytic and dielectric elastomer under equal-biaxial stretch λ may be written as:

$$\tau = \frac{2\varepsilon A_{\mathrm{D}} \rho_{\mathrm{electrolyte}}}{H_{\mathrm{D}} H_{\mathrm{electrolyte}}} \lambda^6, \tag{8}$$

where $\rho_{\mathrm{electrolyte}}$ and $H_{\mathrm{electrolyte}}$ are the resistivity and thickness of the electrolyte, respectively. Thus, $\tau \sim c_{\mathrm{D}} A_{\mathrm{D}} R \lambda^6$, where R is the sheet resistance of the electrolyte. For representative values $c_{\mathrm{D}}=10^{-8}$ F/m^2, $A_{\mathrm{D}}=10^{-2}$ m^2, and $R=10^2$ Ω/sq, we estimate that $\tau \sim 10^{-8}$ s when $\lambda=1$, and $\tau \sim 10^{-6}$ s when $\lambda=2$. This estimate does not include the electrical resistance of the lines of hydrogels between the large pad of the hydrogels and the copper electrodes. If these lines are thin and long, they will dominate the net resistance, and increase the RC delay.

Fundamental resonance due to elasticity and inertia. We estimate the resonant frequency of the actuator by the in-plane vibration of a thin sheet, area A and thickness H. The mass of the sheet is $m=\rho AH$, where ρ is the mass density. The effective

stiffness of the sheet scales as $k \sim YH$, where Y is the elastic modulus. The frequency of the fundamental mode of resonance is $\omega = \sqrt{k/m}$. When the actuator is subject to a cyclic voltage of a certain frequency of excitation Ω, the amplitude of vibration of the actuator is the same as that induced by the static voltage when $\Omega << \omega$, and vanishes when $\Omega >> \omega$ (*35*). Thus, the fundamental resonance sets a time scale, $\tau_{\text{inertia}} = 1/\omega$, for the amplitude of actuation to vanish. This estimate gives $\tau_{\text{inertia}} \sim \sqrt{A_D \rho / Y}$. This estimate is consistent with the observed limiting frequency of actuation. The estimate is also consistent with previous observations for dielectric elastomer actuators made of silicone coated with carbon grease (*36*), where the actuation speed was limited by the resonant frequency of approximately 1 kHz, or $\tau_{\text{inertia}} \approx 10^{-3}$ s for estimated values $A_D = 10^{-2}$ m², $\rho = 10^3$ kg/m³ and $Y = 10^6$ N/m².

Incidentally, a similar estimate also applies to the fundamental resonance of a dielectric elastomer actuator deflecting out of plane, like the membrane of a drum. Because the membrane is pre-stretched substantially, the tension in the membrane scales with the elastic modulus as $T \sim YH$. The frequency of fundamental resonance scales as $\omega = \sqrt{T/m}$. The fundamental mode of resonance sets a time scale, $\tau_{\text{inertia}} = 1/\omega$, which again gives $\tau_{\text{inertia}} \sim \sqrt{A_D \rho / Y}$. This estimate is close to an experimental observation of miniaturized diaphragm dielectric elastomer actuators (*37*), where the limiting frequency of actuation was approximately 1 kHz. Using representative values $A_D \sim 10^{-5}$ m², $\rho \sim 10^3$ kg/m³ and $Y \sim 10^6$ N/m², we find that $\tau_{\text{inertia}} \approx 10^{-4}$ s.

Equilibrium states of layered electrolytic and dielectric elastomers. This calculation assumes a square dielectric membrane, length L and thickness H_o in the undeformed state. The elastomer is taken to be incompressible. The dielectric membrane is prestretched by an equal-biaxial force P to length $\lambda_{\text{pre}} L$ and thickness

$H_1 = H_0\lambda_{\text{pre}}^{-2}$, and then sandwiched between two membranes of an electrolytic elastomer, of combined thickness H_2 in the undeformed state. Subject to both the force P and the voltage V, the sandwich is further stretched to length λL. Dielectric elastomers show pronounced strain-stiffening, and are represented by the Gent model (*38*). In equilibrium, the equation of state takes the form (*39*):

$$\frac{P\lambda}{\lambda_{\text{pre}}^2 L(H_1+H_2)}+\varphi^{\text{A}}\varepsilon\left(\frac{V}{H_0}\right)^2\lambda^4=\frac{\varphi^{\text{A}}\mu^{\text{A}}\left(\lambda^2-\lambda^{-4}\right)}{1-\left(2\lambda^2+\lambda^{-4}-3\right)/J_{\text{lim}}^{\text{A}}}+\frac{\varphi^{\text{B}}\mu^{\text{B}}\left(\lambda^2\lambda_{\text{pre}}^{-2}-\lambda^{-4}\lambda_{\text{pre}}^4\right)}{1-\left(2\lambda^2\lambda_{\text{pre}}^{-2}+\lambda^{-4}\lambda_{\text{pre}}^4-3\right)/J_{\text{lim}}^{\text{B}}}, \qquad (9)$$

Where $\varphi^{\text{A}}=H_1/(H_1+H_2)$, $\varphi^{\text{B}}=H_2/(H_1+H_2)$, ε is the dielectric permittivity, μ^{A} is the shear modulus of the dielectric elastomer, and μ^{B} is the shear modulus of the electrolyte. Similarly, $J_{\text{lim}}^{\text{A}}$ and $J_{\text{lim}}^{\text{B}}$ are the parameters related to the stiffening of the elastomer and the electrodes. Equation (9) defines the stretch of the membrane subject to given values of P and V.

Define the area strain as $\varepsilon_{\text{area}}=(\lambda/\lambda_{\text{pre}})^2-1$. We compare predicted area strain as a function of the voltage to the experimental data for the actuator of a prestretch of $\lambda_{\text{pre}}=3$ (Fig. S2G). A good agreement between theory and experiments is observed, when the shear modulus of the dielectric elastomer is chosen as $\mu^{\text{A}}=34$ kPa, with $J_{\text{lim}}^{\text{A}}=90$. The fitted shear modulus compares well with those reported elsewhere (*40, 41*). For the dielectric elastomer, the permittivity is $\varepsilon=4.11\text{x}10^{-11}$ F/m. The shear modulus of the hydrogel is set to the experimentally determined value of $\mu^{\text{B}}=3$ kPa, and we assume a neo-Hookean stress-strain relation with $J_{\text{lim}}^{\text{B}}=\infty$.

Viscoelasticity of layered electrolytic and dielectric elastomers. Viscoelastic dielectric elastomers can be simulated using rheological models of springs and dashpots (*42*). Here we adopt a model of two polymer networks connected in parallel (Fig. S2H). One network consists of a spring α, and the other network consists of

another spring β connected in series with a dashpot. Subject to a force, the networks deform by a stretch λ. By geometry, the spring α deforms by stretch λ. For the bottom network, the spring β deforms by stretch λ^e, and the dashpot deforms by stretch ξ. The total stretch in the bottom network is given by $\lambda^e\xi$ which must be equal to λ. The equation of motion may be written as:

$$\begin{aligned}&\frac{P\lambda}{\lambda_{\text{pre}}^2 L\left(H_1+H_2\right)}+\varphi^{\text{A}}\varepsilon\left(\frac{V}{H_0}\right)^2\lambda^4\\&=\frac{\varphi^{\text{A}}\mu^{\alpha}\left(\lambda^2-\lambda^{-4}\right)}{1-\left(2\lambda^2+\lambda^{-4}-3\right)/J_{\text{lim}}^{\alpha}}+\frac{\varphi^{\text{A}}\mu^{\beta}\left(\lambda^2\xi^{-2}-\xi^4\lambda^{-4}\right)}{1-\left(2\lambda^2\xi^{-2}+\xi^4\lambda^{-4}-3\right)/J_{\text{lim}}^{\beta}}+\frac{\varphi^{\text{B}}\mu^{\text{B}}\left(\lambda^2\lambda_{\text{pre}}^{-2}-\lambda^{-4}\lambda_{\text{pre}}^4\right)}{1-\left(2\lambda^2\lambda_{\text{pre}}^{-2}+\lambda^{-4}\lambda_{\text{pre}}^4-3\right)/J_{\text{lim}}^{\text{B}}}\end{aligned}\tag{10}$$

Where μ^{α} and μ^{β} are shear moduli of the two springs, and J_{lim}^{α} and J_{lim}^{β} are constants related to the limiting stretches of the two springs. The three terms on the right-hand side of Eq. (10) are the stresses carried by the two springs in the rheological model. We next model the dashpot as a Newtonian fluid. In the rheological model, the state of stress in the dashpot is the same as that in spring β. Consequently, we define the rate of deformation in the dashpot:

$$\frac{\mathrm{d}\xi}{\xi \mathrm{d}t}=\frac{1}{6\eta}\left(\frac{\varphi^{\text{A}}\mu^{\beta}\left(\lambda^2\xi^{-2}-\xi^4\lambda^{-4}\right)}{1-\left(2\lambda^2\xi^{-2}+\xi^4\lambda^{-4}-3\right)/J_{\text{lim}}^{\beta}}\right),\tag{11}$$

where η is the viscosity of the dashpot. With (10) and (11), we solve for λ(t) and ξ(t), once $V(t)$ and $P(t)$ are prescribed. The theoretical model is compared to the experimental data (Fig. S2F). The actuator was subject to a voltage, which was applied suddenly at time zero, and was then held constant subsequently (Fig. S2E). The initial vertical segment and the solid curve are theoretical predictions. In short time, the elastomer behaves as a purely elastic material, and expands instantaneously in response to the sudden jump in the applied voltage. Subsequently, the elastomer expands as a function of time due to

viscoelastic creep. The fitting parameters used are μ^{α}=26 kPa, μ^{β}=110 kPa, $J_{\lim}^{\alpha} = 89$, $J_{\lim}^{\beta} = 30$, and η=0.33 MPas.

Effect of the elasticity of the electrolyte. We show that the voltage-induced deformation is limited by electromechanical instability, and examine the effect of the electrolyte on the instability using equation (9). The electromechanical response of actuators varies with the levels of prestretch λ_{pre} (Fig. S3). Here we use representative values of shear modulus for hydrogels (μ^{B}=3 kPa) and ion gels (μ^{B}=400 kPa) (*19*). For the dielectric, the electric breakdown voltage $V_{EB}=E_{EB}h$, with a constant value of the electric breakdown field set to E_{EB}=200 MV/m.

The hydrogel is less stiff, resulting in a larger actuation strain at the same applied voltage. At λ_{pre}=1, the voltage-stretch curve of the actuator using the hydrogel shows a local maximum before intersecting with the electrical breakdown curve (plotted in red), and the actuator fails by electromechanical instability once the local maximum of the curve is reached. When λ_{pre}=2, the voltage-stretch curve for the hydrogel electrolyte becomes monotonic. Consequently, the maximum actuation strain is limited by electric breakdown. By eliminating instability, the membrane is able to achieve large actuation strain. The transition from the occurrence of electromechanical instability to stable behavior occurs at $\lambda_{pre}\approx1.93$. The ion gel is stiffer, so that larger pre-stretches are required to avert instability; the transition occurs at $\lambda_{pre}\approx3.24$. Even in the stable region, the achievable strain at electrical breakdown is lower for the stiffer electrodes. Therefore the actuator may achieve large actuation strains for a small electrolyte modulus and a λ_{pre} large enough to avert instability. Increasing the stiffness of the electrolyte of an actuator operating in the electromechanically stable regime may render it unstable.

High-speed, long-distance ionic interconnects. In the actuator and loudspeaker, we connect the active regions of the devices to the copper electrodes using thin lines of ionic conductors. This design demonstrates that ionic conductors can be used as high-speed, stretchable and transparent interconnects. The ionic conductors have much higher electrical resistance than typical electronic conductors; for example, the resistivity of our hydrogels is $\rho \sim 10^{-2}$ Ωm, and the resistivity of copper is $\rho \sim 10^{-8}$ Ωm. How fast and how far can a signal propagate along the ionic interconnects? The answers depend on the resistivity of the conductor and the permittivity of the surrounding insulators, as well as on the geometry of the setup. To gain some insight, here we use an idealized model for the propagation of potentials along myelinated axons (*43*).

In this model, a conducting line is inside a dielectric sheath, which is surrounded by another conductor (Fig. S8). The outside conductor is grounded. The conducting line and the dielectric sheath are a resistor and a capacitor. As an electric current propagates along the resistor, part of the electric charge is deposited to the capacitor. Let x be the distance from one end along the length of the resistor. At time t, let $I(x,t)$ be the electric current along the length of the resistor, and $Q(x,t)$ be the electric charge per unit length of the capacitor. The conservation of electric charge requires that

$$\frac{\partial Q}{\partial t} + \frac{\partial I}{\partial x} = 0 . \tag{12}$$

Let $V(x,t)$ be the electric potential in the resistor. Ohm's law requires that

$$\frac{\partial V}{\partial x} = -rI , \tag{13}$$

where r is the resistance per unit length of the conducting line. Because the outside conductor is grounded, V is also the voltage across the thickness of the capacitor, so that

$$Q = cV , \tag{14}$$

where c is the capacitance per unit length of the dielectric.

Combining (12)-(14) gives that

$$\frac{\partial V}{\partial t} = \frac{1}{rc}\frac{\partial^2 V}{\partial x^2}. \tag{15}$$

This is a diffusion equation, with the effective diffusivity

$$D = \frac{1}{rc}. \tag{16}$$

Consider a conducting line of circular cross section of radius a inside of a dielectric sheath of external radius b. The resistance per unit length of the conducting line is

$$r = \frac{\rho}{\pi a^2}, \tag{17}$$

where ρ is the resistivity of the conductor. The capacitance per unit length of the dielectric sheath is

$$c = \frac{2\pi\varepsilon}{\log(b/a)}, \tag{18}$$

where ε is the permittivity of the dielectric.

In the following estimates, we drop factors of order unity. Using (16)-(18), we find that the effective diffusivity scales as

$$D \sim \frac{a^2}{\rho\varepsilon}. \tag{19}$$

The product $\rho\varepsilon$ is a time scale specific to the materials, and is independent of the geometry of the setup. For a conductor of $\rho \approx 10^{-2}$ Ωm, and a dielectric of permittivity $\varepsilon \approx 10^{-11}$ F/m, we obtain that $\rho\varepsilon \sim 10^{-13}$ s.

When a step voltage is suddenly applied at one end of the interconnect, the signal takes some time to reach the other end. For an interconnect of length L, the delay time scales as $\tau \sim L^2/D$, namely,

$$\tau \sim \rho\varepsilon(L/a)^2. \tag{20}$$

For an interconnect of radius a=10^{-4} m and length L=10^{-1} m, the delay time is τ~10^{-7} s.

When a sinusoidal voltage of frequency ω is applied at one end of the interconnect, the amplitude of the voltage decays as the signal propagates along the interconnect. The decay length scales as $L \sim \sqrt{D/\omega}$, namely,

$$L \sim \frac{a}{\sqrt{\rho\varepsilon\omega}}. \tag{21}$$

For an interconnect of radius a=10^{-4} m and a signal of frequency ω=10^{5} Hz, the decay length is L~1 m.

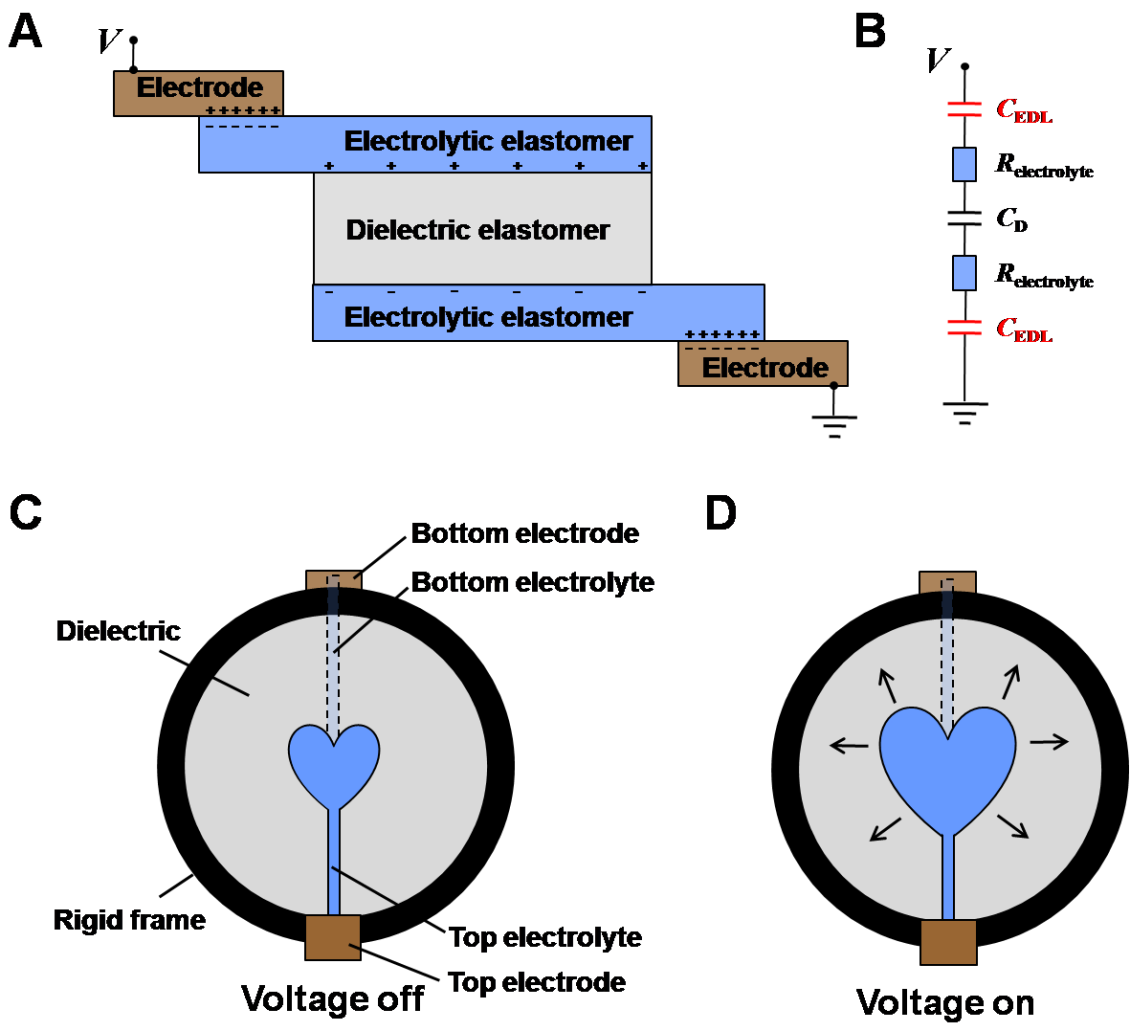

Fig. S1. Layered electrolytic and dielectric elastomer, a design of stretchable ionics that enables electromechanical functions without electrochemical reaction. (**A**) A layer of a dielectric elastomer is sandwiched between two layers of an electrolytic elastomer. The electrodes are placed outside the active region of the device, so that the device is stretchable and transparent. (**B**) Equivalent circuit of the device. **(C)** A specific design of an actuator with the electrolyte in the shape of a heart. **(D)** The heart expands when the voltage is applied.

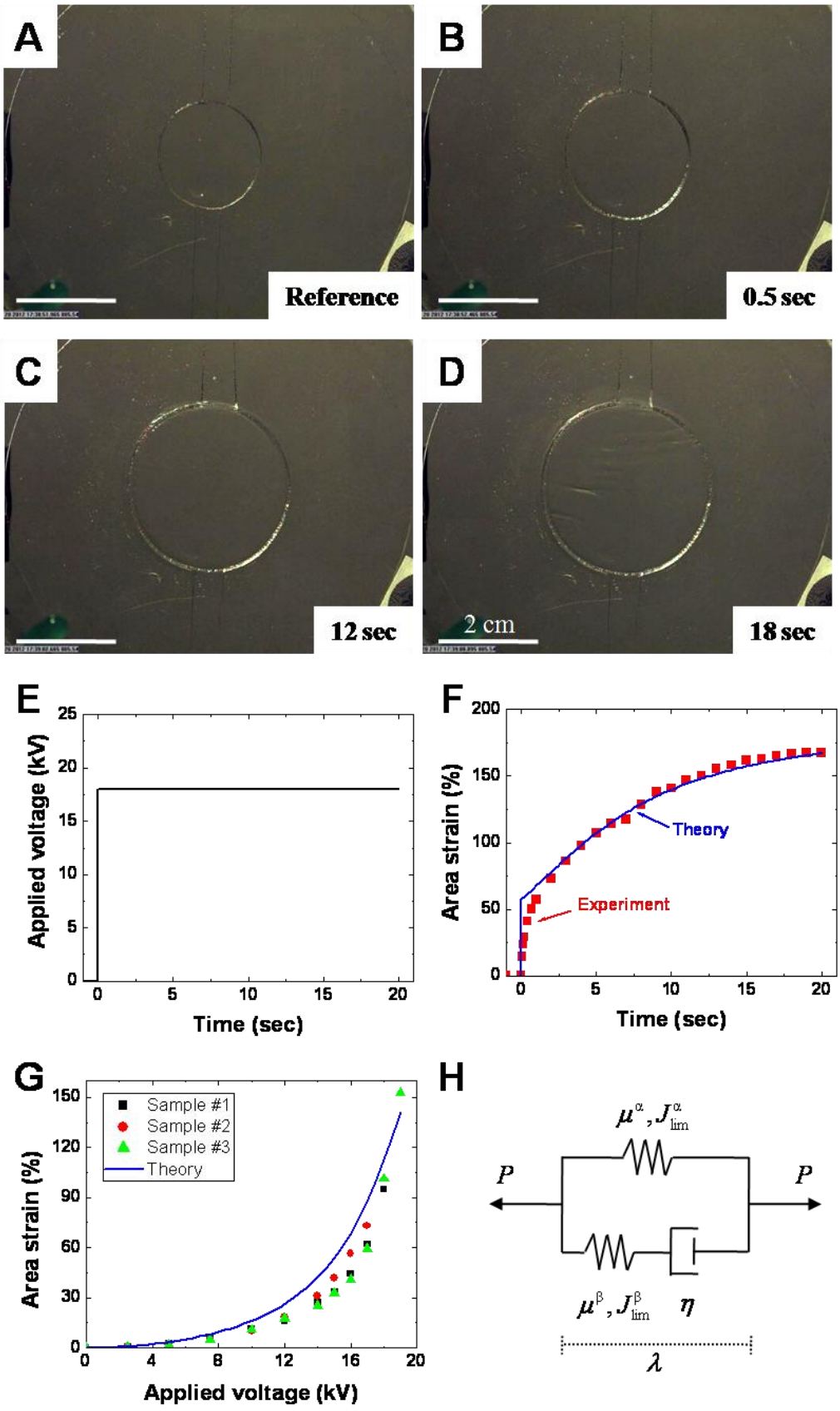
A
Reference
B
0.5 sec
C
12 sec
D
2 cm
18 sec
E
Applied voltage (kV)
Time (sec)
F
Area strain (%)
Theory
Experiment
Time (sec)
G
Sample #1
Sample #2
Sample #3
Theory
Area strain (%)
Applied voltage (kV)
H
$\mu^{\alpha}, J_{\lim}^{\alpha}$
P
P
$\mu^{\beta}, J_{\lim}^{\beta}$
η
λ

Fig. S2. Actuator using hydrogels of circular shape. **(A)-(D)** When a voltage was suddenly applied and subsequently held constant, the actuator expanded in area over time. **(E)** At time zero, a voltage of 18 kV is rapidly applied, and is then held constant. **(F)** The area strain is measured as a function of time, and the experimental data are compared with the theoretical prediction. **(G)** The area strain measured at 20 s after the voltage is applied. **(H)** The viscoelasticity of the dielectric elastomer is represented by a rheological model of two parallel units: the top unit consists of spring α, and the bottom unit consists of spring β in series with a dashpot.

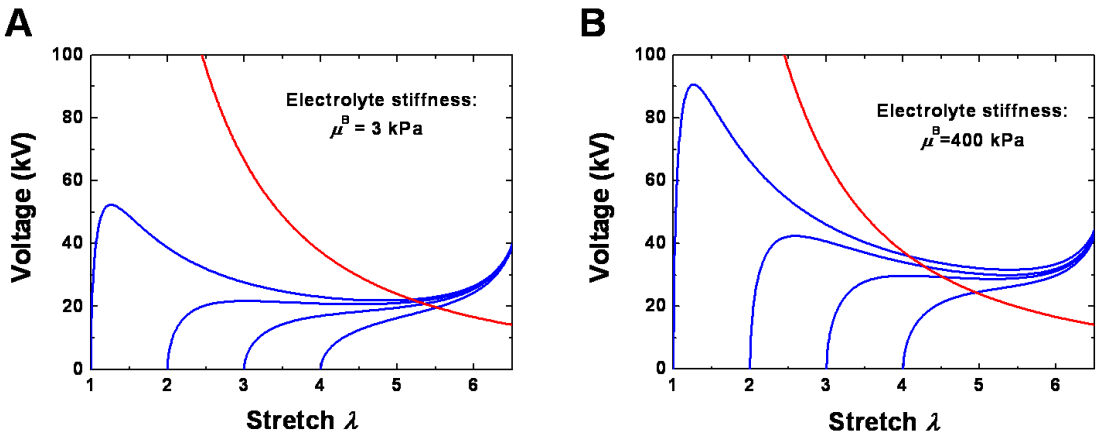

Fig. S3. Theoretical voltage-stretch curves of actuators with different levels of pre-stretch. The red curves correspond to the electric breakdown field of 200 MV/m. **(A)** The electrolyte is a hydrogel with a shear modulus of 3 kPa. **(B)** The electrolyte is an ion gel with a shear modulus of 400 kPa.

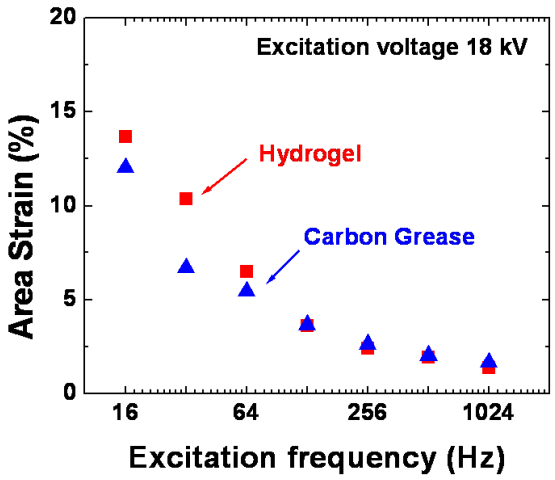

Fig. S4. An actuator using carbon grease as the conductor is compared with an actuator using the hydrogel as the conductor. The area-frequency curves of the two actuators are nearly indistinguishable.

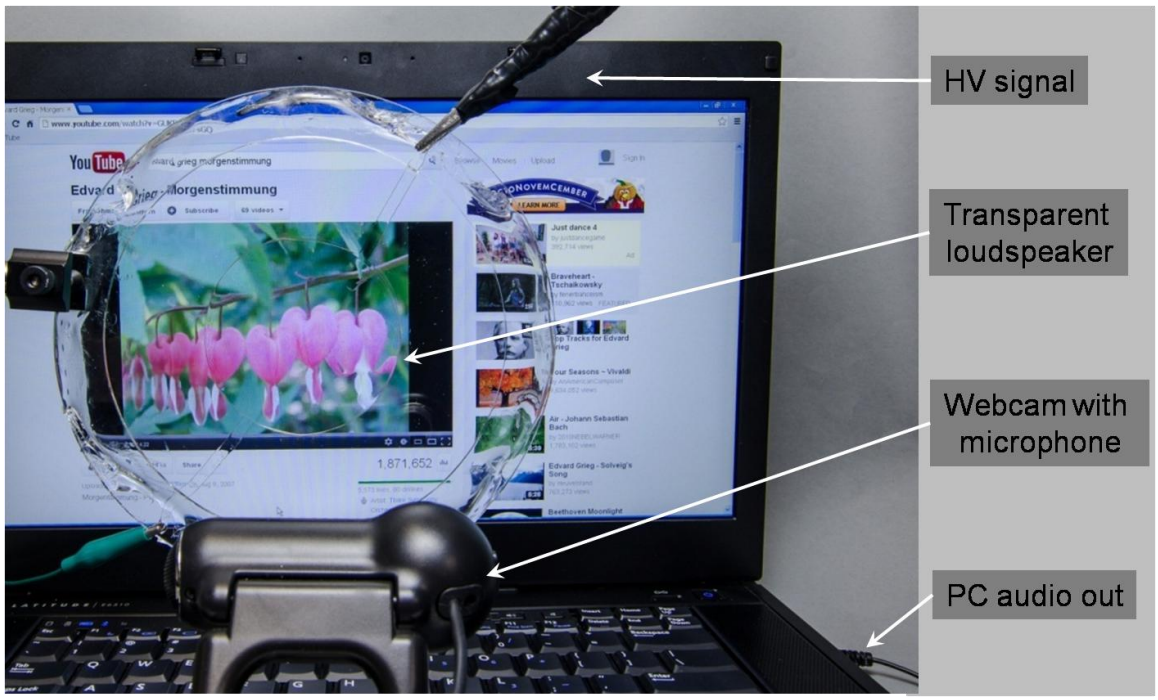

Fig. S5. The experimental setup for the transparent loudspeaker. The loudspeaker is placed in front of a laptop playing a music video. The video is clearly visible through the loudspeaker. The sound track of the video is fed to the loudspeaker as a high-voltage signal, from the audio output of the laptop, through a high voltage amplifier. A microphone records the sound produced by the loudspeaker.

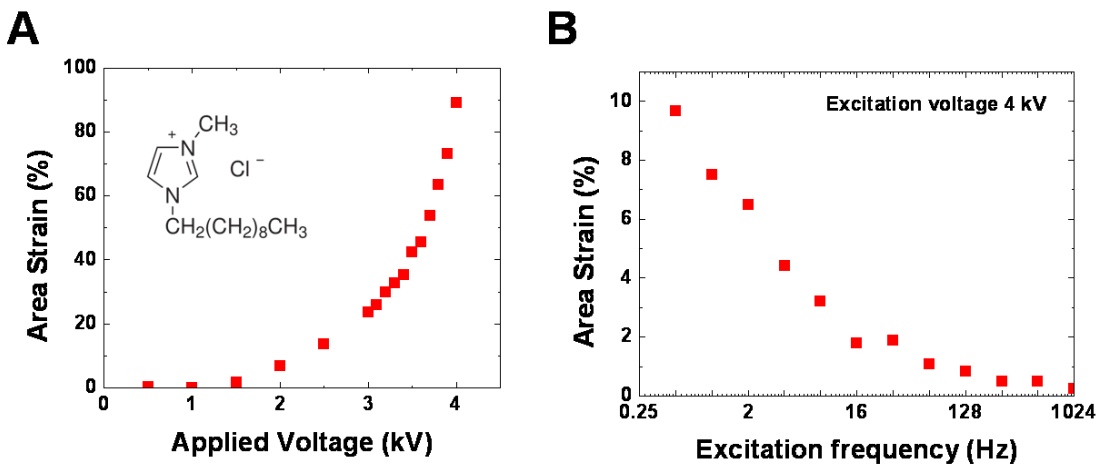

Fig. S6. Performance of a dielectric elastomer actuator using an ionic liquid as the conductor. **(A)** Area strain of an actuator using the ionic liquid [C10MIM][Cl] as conductor as a function of applied voltage. **(B)** Area strain measured as a function of excitation frequency at an applied voltage of 4 kV.

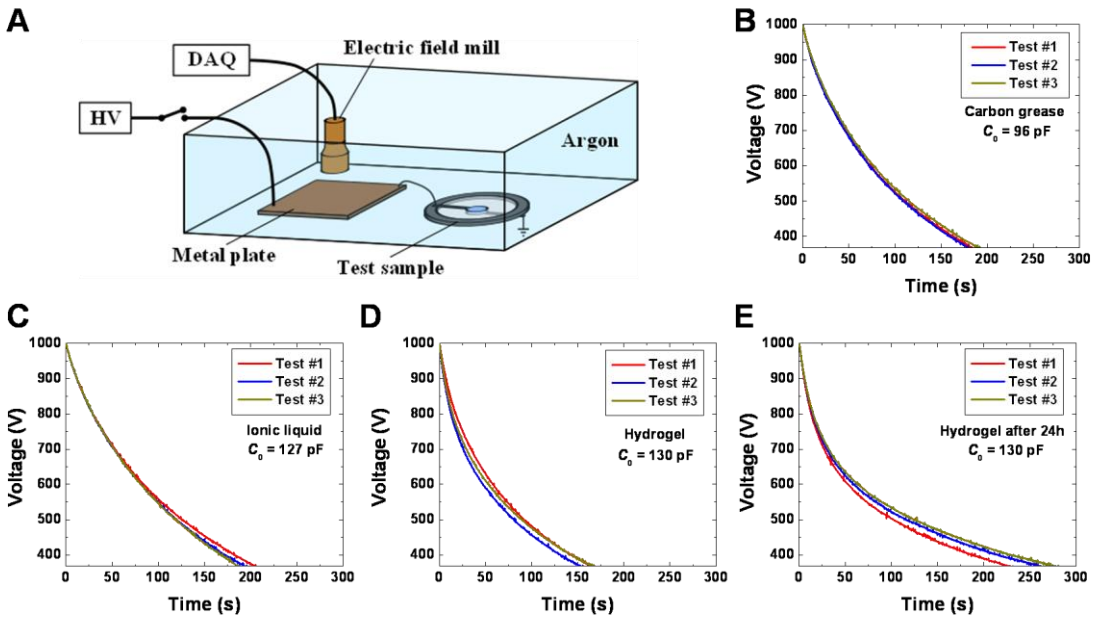

Fig. S7. Charge leakage through a dielectric when conductors of several types are used. **(A)** An electric field mill is used for contactless measurement of the electrical potential of a metal plate which is connected to a test sample. **(B)-(D)** Experimental results on the decrease of electrical potential over time for electrodes based on carbon grease, ionic liquid and hydrogel. **(E)** Test results for the same hydrogel sample used in **(D)** after 24 h of storage time.

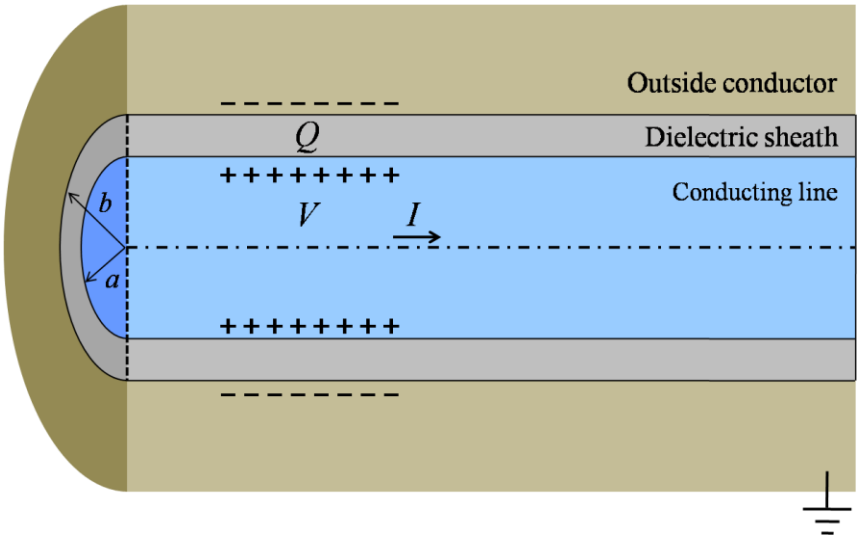

Fig. S8. Propagation of an electrical signal along the length of an interconnect. A conducting line is inside a dielectric sheath, which is surrounded by another conductor. The outside conductor is grounded.

Movie S1

Transparent actuator beating at a frequency of 1 Hz (excitation voltage 17 kV). The green LED in the left bottom corner of the video indicates voltage on (LED off) and voltage off (LED on).

Movie S2

Transparent loudspeaker playing music in front of the screen of a laptop.

Movie S3

Recording of the transparent loudspeaker playing a linear sine sweep from 20 Hz to 20 kHz within 20 s.

Movie S4

Side view recording of the transparent loudspeaker playing a logarithmic sine sweep from 20 Hz to 20 kHz within 100 s. Vibrations of the frame and out-of-plane standing wave patterns of the transparent membrane are visible in the low-frequency range.